Molecular Crystals and Liquid Crystals

ISSN: 1542-1406 (Print) 1563-5287 (Online) Journal homepage: http://www.tandfonline.com/loi/gmcl20

Synthesis of a BDT-based small-molecule acceptor with dye end groups for organic photovoltaic cell application

Eunhee Lim

To cite this article: Eunhee Lim (2016) Synthesis of a BDT-based small-molecule acceptor with dye end groups for organic photovoltaic cell application, Molecular Crystals and Liquid Crystals, 635:1, 94-101, DOI: 10.1080/15421406.2016.1200368

To link to this article: http://dx.doi.org/10.1080/15421406.2016.1200368

MOLECULAR CRYSTALS AND LIQUID CRYSTALS
2016, VOL. 635, 94–101
http://dx.doi.org/10.1080/15421406.2016.1200368

Taylor & Francis
Taylor & Francis Group

Synthesis of a BDT-based small-molecule acceptor with dye end groups for organic photovoltaic cell application

Eunhee Lim

Department of Chemistry, Kyonggi University, Gyeonggi, Republic of Korea

ABSTRACT

An acceptor-donor-acceptor (A–D–A)-type small molecule, **BDT-IN**, having a benzo[1,2-*b*:4,5-*b*′]dithiophene (BDT) unit as its electron-donating core (D) and an 1,3-indanedione (IN) unit as its electron-withdrawing end group (A), was synthesized by Knoevenagel condensation. The **BDT-IN** film showed broader UV absorption with a greater red shift (λ_{max} = 622 nm) than that of the **BDT-IN** solution (λ_{max} = 570 nm). The organic photovoltaic cells were fabricated with an ITO/PEDOT:PSS/poly(3-hexylthiophene): **BDT-IN**/LiF/Al configuration, and showed a power conversion efficiency of 0.23%.

KEYWORDS

Organic photovoltaic cells; OPV; benzo[1,2-*b*:4,5-*b*′]dithiophene (BDT); 1,3-indandione

1. Introduction

During the last decade, organic photovoltaic cells (OPVs) have attracted much interest because of advantages such as light weight, low cost, and flexibility [1]. Much effort has been devoted to develop polymer and small-molecule electron donors for bulk heterojunction OPVs. To date, high power conversion efficiencies (PCEs) of 10.6% [2] and 10.1% [3] have been achieved with tandem devices based on polymer and small-molecule donors, respectively, blended with fullerene derivatives as acceptors. At the same time, the importance of non-fullerene acceptors has also been emphasized owing to their high absorption of sunlight, easy synthesis, and adjustable frontier orbital energy levels. The highest PCE (5.9%) has been reported for a non-fullerene acceptor based on perylenediimide (PDI) [4].

Recently, various dyes such as alkyl cyanoacetate, 3-ethylrhodanine, and 1,3-indanedione (IN) have been introduced as terminal end groups. In particular, the IN dye unit, with its high electron-accepting ability and good planar structure, has been much used as an electron-withdrawing end group, resulting in low band-gap small-molecule donors and acceptors [5, 6]. Up to 6.75% of performance has been achieved for devices based on small-molecule donors having IN dye end groups [5]. Recently, Watkins et al and our research team independently reported A-D-A-type small molecules containing IN end groups for the use as acceptors in non-fullerene OPVs [7, 8]. The device performance varied with the introduction of electron-donating cores (D). The fluorene-IN-based small-molecule Flu-IN exhibited high PCEs of up to 1.52%, whereas Cz-IN, based on carbazole and IN, showed a low device performance because of excessively strong aggregation.

CONTACT Eunhee Lim ehlim@kyonggi.ac.kr
Color versions of one or more of the figures in the article can be found online at www.tandfonline.com/gmcl.

The well-known electron-donating unit benzo[1,2-*b*:4,5-*b'*]dithiophene (BDT) has a symmetric and planar conjugated structure that can easily realize the ordered $\pi-\pi$ stacking and facilitate high charge transport [9]. The devices, based on polymer and small-molecule donors composed of a BDT backbone, showed record efficiencies of over 10% [3, 10]. In addition, the introduction of suitable strong electron-withdrawing moieties such as PDI and 4,4-difluoro-4-bora-3*a*,4*a*-diaza-*s*-indacene onto the BDT cores made them good candidates for non-fullerene acceptors with high PCEs of over 1% [8, 11].

In this study, we synthesized the IN end-capped BDT-based small-molecule **BDT-IN** as an acceptor for non-fullerene OPVs. Physical properties of **BDT-IN**, such as optical and electrochemical properties, were investigated and compared with those of other IN-containing small-molecule acceptors (Cz-IN and Flu-IN).

2. Experimental

2.1. Materials

BDT, 5-formyl-2-thiophene boronic acid, and IN were purchased from TCI. 2-Ethylhexylbromide, tetrabutylammonium bromide (TBAB), tris(dibenzylideneacetone) dipalladium(0) ($Pd_2(dba)_3$), tri-*tert*-butylphosphonium tetrafluoroborate ($P(t\text{-}Bu)_3 \times HBF_4$), potassium phosphate ($K_3PO_4$), and *tert*-butanol were purchased from Aldrich. Zinc powder was purchased from SHOWA. Bromine was purchased from JUNSEI. All reagents purchased commercially were used without further purification, except for tetrahydrofuran (THF) solvent that was dried over a sodium/benzophenone mixture. The compounds 4,8-bis(2-ethylhexyloxy)benzo[1,2-*b*:3,4-*b*]dithiophene (**1**), 2,6-dibromo-4,8-bis(2-ethylhexyl)benzo[1,2-b:3,4-b]dithiophene (**2**), and 2,6-diformyl-4,8-bis(2-ethylhexyl)benzo[1,2-*b*:3,4-*b*]dithiophene (**3**) were prepared according to literature [12].

2.2. Physical measurements

NMR spectra were recorded on a Bruker AVANCE III HD 400 spectrometer. UV-vis spectra were obtained using a Shimadzu UV/vis spectrometer. The electrochemical properties of the small molecule were characterized by cyclic voltammetry (CV) with a BAS 100B electrochemical analyzer, and calibrated using a ferrocenium/ferrocene redox value of −4.8 eV as the standard. A three-electrode system was used, consisting of a non-aqueous reference electrode (0.1 M Ag/Ag^+ acetonitrile solution), a platinum working electrode, and a platinum wire as a counter electrode. The redox potential of the small molecules was measured in acetonitrile with 0.1 M $(n\text{-}C_4H_9)_4N\text{-}PF_6$. The films were prepared by dip-coating the small molecule solutions onto the platinum working electrode, and measurements were calibrated using the ferrocene value (−4.8 eV) as the standard. Atomic force microscopy (AFM) images were obtained with a Scanning Probe Microscope (XE-100) by Park Systems. The AFM measurements were performed on the same samples that were used in the OPV devices as the top layer of the device (ITO/PEDOT:PSS/P3HT:**BDT-IN**/LiF/Al).

2.3. Synthesis

2.3.1. Synthesis of compound (1)

NaOH (15 g) was added to BDT (5.1 g, 23 mmol), zinc powder (3.3 g, 51 mmol), and 80 mL of water in a 250 mL flask, and the mixture was refluxed for 1 h. A catalytic amount of TBAB and

2-ethylhexylbromide (13 g, 70 mmol) were then added, and the resulting mixture was refluxed for a further 6 h. The crude product was extracted with diethyl ether and water, dried over $MgSO_4$, and purified by silica gel chromatography using dichloromethane:hexane (1:5) as an eluent. A colorless sticky oil was obtained as the final product (7.25 g, yield 70%). ^{1}H NMR ($CDCl_3$, 400 MHz): δ (ppm) 7.67 (d, 2 H), 7.37 (d, 2 H), 4.19 (d, 4 H), 1.7 (m, 2 H), 1.6–1.4 (m, 16 H), 1.08 (t, 6 H), 0.92 (t, 6 H).

2.3.2. Synthesis of compound (2)

A solution of bromine (5.1 g, 64 mmol in 48 mL dichloromethane) was slowly dropped into a solution of compound (**1**) (7.3 g, 10 mmol in 240 mL dichloromethane) cooled in an ice-water bath. Subsequently, the reactants were stirred overnight at room temperature so that the color of the bromine diminished. The solvent was then evaporated under vacuum, and the resulting residue was purified by silica gel chromatography with hexane as eluent. A colorless sticky oil was obtained as the final product (5.5 g, yield 56%). ^{1}H NMR ($CDCl_3$, 400 MHz): δ (ppm) 7.42 (s, 2H), 4.19 (d, 4H), 1.7 (m, 2H), 1.6–1.4 (m, 16H), 1.08 (t, 6H), 0.92 (t, 6H).

2.3.3. Synthesis of compound (3)

Compound (**2**) (0.90 g, 1.5 mmol), 5-formyl-2-thiophene boronic acid (0.97 g, 5.9 mmol), $Pd_2(dba)_3$ (0.036 g, 0.040 mmol), and P(*t*-Bu)$_3$ × HBF_4 (0.022 g, 0.080 mmol) were dissolved in THF (30 mL). A solution of K_3PO_4 (1.2 g, 5.6 mmol) dissolved in 3.1 mL H_2O was added, and the mixture was heated overnight at 90°C. The crude product was extracted with dichloromethane and water, dried over $MgSO_4$, and purified by recrystallization from ethanol. A dark solid was obtained as the final product (0.86 g, yield 89%). ^{1}H NMR (400 MHz, $CDCl_3$): δ (ppm) 9.92 (s, 2H), 7.74 (d, 2H), 7.89 (s, 2H), 7.41 (d,2H), 4.19 (d, 4H), 1.7 (m, 2H), 1.6–1.4 (m, 16H), 1.08 (t, 6H), 0.92 (t, 6H).

2.3.4. Synthesis of BDT-IN

Three drops of piperidine were added to a solution of compound (**3**) (0.50 g, 0.77 mmol) and IN (0.34 g, 2.3 mmol) in *tert*-butanol (17 mL). The resulting solution was stirred under reflux for 24 h and cooled to 50°C. Ethanol (8.5 mL) was then added, and the reaction was further cooled to room temperature. The precipitate was filtered, washed with ethanol, and purified by silica gel chromatography using chloroform:hexane (1:1) as the eluent. A dark solid was obtained as the final product (48 mg, yield 7.0%). ^{1}H NMR ($CDCl_3$, 400 MHz): δ (ppm) 8.00–8.05 (m, 8H), 7.80–7.87 (m, 4H), 7.47 (m, 2H), 4.19 (d, 4H), 1.7 (m, 2H), 1.6–1.4 (m, 16H), 1.08 (t, 6H), 0.92 (t, 6H).

2.4. Fabrication of OPV devices

The OPVs were fabricated with an ITO/PEDOT:PSS/poly(3-hexylthiophene) (P3HT):**BDT-IN** (1:1.5)/LiF/Al configuration. After filtering through a 0.45 μm PTFE membrane syringe, a chloroform solution of P3HT and **BDT-IN** was spin-coated at 3000 rpm. A LiF/Al layer was then deposited on the active layer. The current–density versus voltage (*J*–*V*) curves were measured using a Keithley 236 source measure unit in air under AM 1.5 G illumination (100 mWcm^{-2}). The external quantum efficiency (EQE) was measured using a reflective microscope objective to focus the light output from a 100 W halogen lamp, outfitted with a monochromator and an optical chopper.

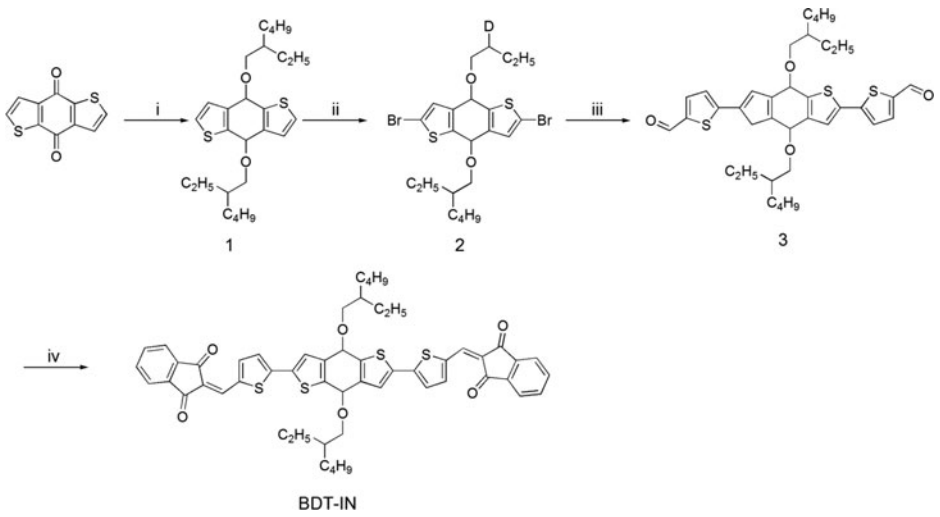

Scheme 1. Synthetic schemes of **BDT-IN**: (i) zinc powder, NaOH, H_2O, reflux, 1 h; followed by 2-ethylhexylbromide, TBAB, reflux, 2 h; (ii) bromine, dichloromethane, room temperature, 12 h; (iii) 5-formyl-2-thiophene boronic acid, $Pd_2(dba)_3$, $P(t\text{-}Bu)_3 \times HBF_4$, K_3PO_4, THF, H_2O; (iv) IN, piperidine, *tert*-butanol, 80°C.

3. Results and discussion

3.1. Synthesis and physical properties

A BDT-based small molecule (**BDT-IN**) was synthesized for use as an acceptor in OPVs. Initially, the ethylhexyloxy-substituted BDT, compound (**1**), was synthesized in two steps. After bromination, compound (**3**) was synthesized by the Suzuki coupling reaction between the brominated BDT, compound (**2**), and 5-formyl-2-thiophene boronic acid. Finally, **BDT-IN** was synthesized by Knoevenagel condensation between compound (**3**) and the IN dye group. The synthetic routes are shown in Scheme 1.

Figure 1 shows the UV absorption spectra of **BDT-IN** in chloroform solution and as a spin-coated thin film. Compared to the absorption spectra of **BDT-IN** in solution (λ_{max} =

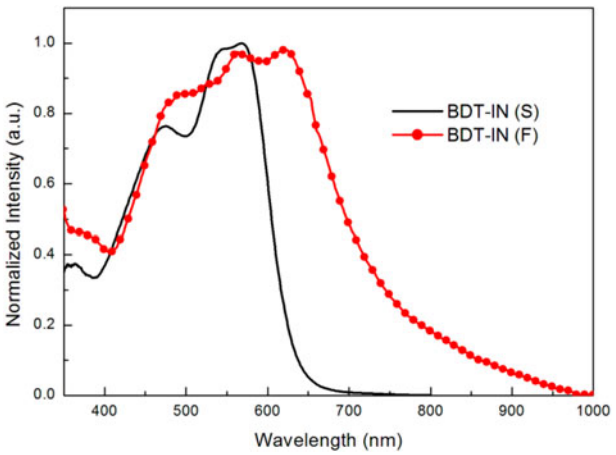

Figure 1. UV-vis absorption spectra of **BDT-IN** in solution (S) and film (F).

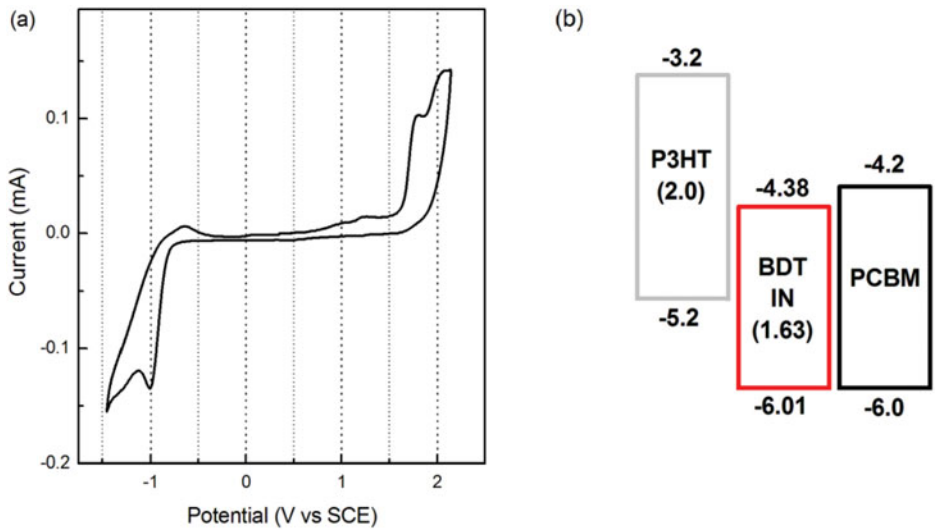

Figure 2. (a) CV curve and (b) energy diagram of **BDT-IN** together with P3HT and $PC_{61}BM$.

570 nm), the **BDT-IN** film ($\lambda_{max} = 622$ nm) showed relatively broader and remarkably red-shifted absorption ($\Delta\lambda = 52$ nm), indicative of the intramolecular charge transfer interactions between the BDT donor and IN acceptor units [13]. A similar but larger red shift ($\Delta\lambda = 58$ nm) was observed in our previous work on IN-based small-molecule acceptor of Cz-IN. In that study, Cz-IN showed a well-structured film absorption with a maximum at 577 nm. Such a phenomenon was explained by the strong molecular aggregation between the Cz-IN molecules, induced by the introduction of the IN end groups. In addition, the absorption spectra of BDT, both in solution and film, are red-shifted when compared to the corresponding spectra of Flu-IN and Cz-IN. Therefore, the optical band gap (E_g) of **BDT-IN**, calculated from the onset of absorption ($\lambda_{onset} = 760$ nm) of the UV-vis spectrum of the film ($E_g = 1240/\lambda_{onset}$ (eV)), was as low as 1.63 eV.

The electrochemical properties of the small molecule were characterized by CV measurements (Figure 2). In the anodic scan, the onset of the oxidation (E_{onset}) of **BDT-IN** occurs at 1.62 eV (vs. SCE). From this, the HOMO energy level of **BDT-IN** was calculated to be −6.01 eV using the empirical relationship proposed by Leeuw et al.: (I_p(HOMO) = -(E_{onset} + 4.39) (eV)) [14]. Interestingly, **BDT-IN** had a much lower HOMO energy level than Cz-IN (−5.57 eV) and Flu-IN (−5.70 eV). The lowest unoccupied molecular orbital (LUMO) energy level of **BDT-IN** was estimated to be −4.38 eV from the optical E_g and the HOMO energy level. This value is sufficiently lower than that of P3HT (−3.2 eV), and can therefore provide a sufficiently large offset between the two LUMO energy levels of P3HT and **BDT-IN** for efficient charge transfer in the P3HT:**BDT-IN** OPV film. In addition, the LUMO energy level of **BDT-IN** was also lower than those of Cz-IN (−3.57 eV) and Flu-IN (−3.63 eV). The optical and electrochemical properties of **BDT-IN** are summarized in Table 1.

3.2. Organic photovoltaic properties

The OPVs were fabricated with an ITO/PEDOT:PSS/P3HT:**BDT-IN**/LiF/Al configuration. The active layer was spin-coated from a chloroform solution of **BDT-IN** and P3HT. The *J*–*V* and EQE curves measured in air under white light AM 1.5 G illuminations (100 mW/cm^2) are shown in Figures 3a and 3b, respectively. The photovoltaic properties of the blend film

Table 1. Physical properties of **BDT-IN**.

	λ_{max} (nm)		E_g [a]	HOMO	LUMO[b]
BDT-IN	solution	film	(eV)	(eV)	(eV)
	570	622	1.63	−6.01	−4.38

[a] E_g was calculated from the onset of absorption of the UV-vis spectrum of the film ($E_g = 1240/\lambda_{onset}$ (eV)).
[b] LUMO was estimated using the HOMO level and E_g.

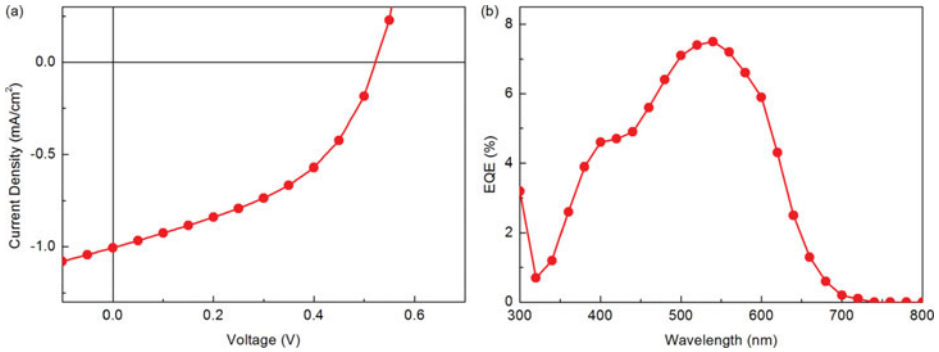

Figure 3. (a) *I-V* and (b) EQE curves of P3HT:**BDT-IN** blend film.

are shown in Table 2. When combined with the P3HT donor, **BDT-IN** (PCE = 0.23%) can be used as an acceptor because of the electron-withdrawing ability of its two terminal IN groups. When compared to other IN-based acceptors of similar structure, the device performance of P3HT:**BDT-IN** was lower than that of the P3HT:Flu-IN device (1.32%), but higher than that of the P3HT:Cz-IN device (0.02%). Unfortunately, the device based on **BDT-IN** showed a lower V_{OC} value (0.54 V) than both Cz-IN (0.61 eV) and Flu-IN (0.92 V). This was caused by a relatively low-lying **BDT-IN** LUMO level (−4.38 eV) when compared to those of both Cz-IN (−3.57 eV) and Flu-IN (−3.63 eV), as stated above. In general, the V_{OC} values are strongly dependent on the energy difference between the HOMO of the donor and the LUMO of the acceptor [15]. In addition, despite a very low band-gap of 1.63 eV in **BDT-IN**, the P3HT:**BDT-IN** device showed a J_{SC} value of only 0.97 mA/cm^2 with a low maximum EQE response of 7% at 540 nm. However, it is worth noting that the P3HT:**BDT-IN** device had an EQE response for longer wavelengths (up to 670 nm) when compared to both P3HT:Flu-IN and P3HT:Cz-IN. These results are well-matched with the relatively red-shifted UV absorption of the **BDT-IN** film, and indicative of the contribution of **BDT-IN** to the photocurrent of the devices. In addition, AFM study showed that the P3HT:**BDT-IN** film a very smooth and homogeneous morphology with root-mean-square surface roughness of 1.0 nm (Figure 4).

Table 2. Photovoltaic properties of P3HT:**BDT-IN** blend films[a].

T_a (°C)[b]	V_{OC} (V)	J_{SC} (mA/cm^2)	FF (%)	PCE (%)
80	0.53	0.84	43	0.19
110	0.54	0.97	44	0.23
140	0.52	1.01	44	0.23

[a] ITO/PEDOT:PSS/P3HT:**BDT-IN**/LiF/Al.
[b] T_a: Annealing temperature.

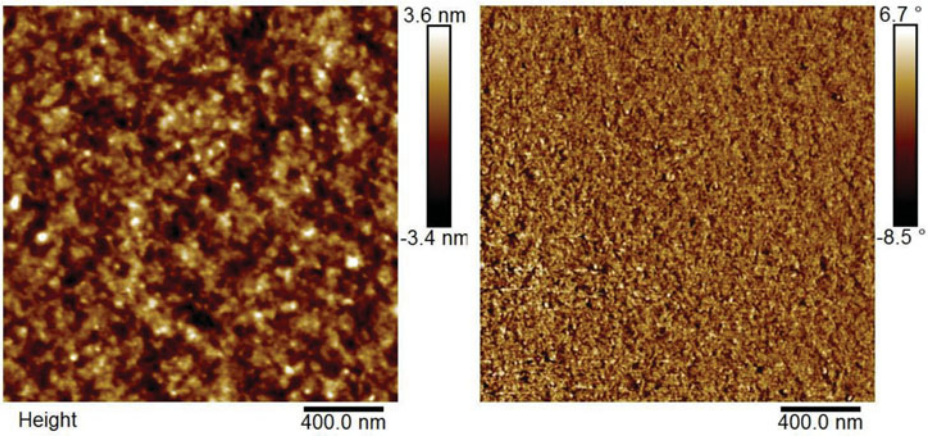

Figure 4. AFM topography (left) and phase image (right) of the P3HT:**BDT** blend films.

Therefore, further optimization by using other donor materials (instead of P3HT) and alternative device architectures as well as the structural modification by introducing other dye end groups could improve device performance.

4. Conclusions

We synthesized an A–D–A-type BDT-based small molecule having IN dye end groups using Knoevenagel condensation, and investigated its optical and electrochemical properties as well as its photovoltaic performance. The introduction of the electron-withdrawing IN end groups made **BDT-IN** suitable as an acceptor in the P3HT:**BDT-IN** OPV film. The OPV device based on **BDT-IN** and P3HT exhibited a PCE of 0.23%. This was an intermediate value between Flu-IN (1.32%) and Cz-IN (0.02%), both of which have IN end groups of similar structure.

Acknowledgments

This work was supported by Kyonggi University Research Grant 2014.

References

[1] Dou, L., You, J., Hong, Z., Xu, Z., Li, G., Street, R. A., & Yang, Y. (2013). *Adv. Mater.*, *25*, 6642.
[2] You, J., Dou, L., Yoshimura, K., Kato, T., Ohya, K., Moriarty, T., Emery, K., Chen, C.-C., Gao, J., Li, G., & Yang, Y. (2013). *Nat. Commun.*, *4*, 1446.
[3] Liu, Y., Chen, C.-C., Hong, Z., Gao, J., Yang, Y., Zhou, H., Dou, L., & Li, G. (2013). *Sci. Rep.*, *3*, 3356.
[4] Zang, Y., Li, C.-Z., Chueh, C.-C., Williams, S. T., Jiang, W., Wang, Z.-H., Yu, J.-S., & Jen, A. K. Y. (2014). *Adv. Mater.*, *26*, 5708.
[5] Shen, S., Jiang, P., He, C., Zhang, J., Shen, P., Zhang, Y., Yi, Y., Zhang, Z., Li, Z., & Li, Y. (2013). *Chem. Mater.*, *25*, 2274.
[6] Tang, W., Huang, D., He, C., Yi, Y., Zhang, J., Di, C., Zhang, Z., & Li, Y. (2014). *Org. Electron.*, *15*, 1155.
[7] Kim, Y., Song, C. E., Moon, S.-J., & Lim, E. (2015). *RSC Adv.*, *5*, 62739.
[8] Poe, A. M., Della Pelle, A. M., Subrahmanyam, A. V., White, W., Wantz, G., & Thayumanavan, S. (2014). *Chem. Commun.*, *50*, 2913.
[9] Gao, C., Wang, L., Li, X., & Wang, H. (2014). *Polym. Chem.*, *5*, 5200.

[10] Zheng, Z., Zhang, S., Zhang, M., Zhao, K., Ye, L., Chen, Y., Yang, B., & Hou, J. (2015). *Adv. Mater.*, *27*, 1189.
[11] Jiang, B., Zhang, X., Zhan, C., Lu, Z., Huang, J., Ding, X., He, S., & Yao, J. (2013). *Polym. Chem.*, *4*, 4631.
[12] Hou, J., Chen, H. -Y., Zhang, S., & Yang, Y. (2009). *J. Phys. Chem. C.*, *113*, 21202.
[13] Lim, N., Cho, N., Paek, S., Kim, C., Lee, J. K., & Ko, J. (2014). *Chem. Mater.*, *26*, 2283.
[14] De Leeuw, D. M., Simenon, M. M. J., Brown, A. R., & Einerhand, R. E. F. (1997). *Synthetic Met.*, *87*, 53.
[15] Scharber, M. C., Mühlbacher, D., Koppe, M., Denk, P., Waldauf, C., Heeger, A. J., & Brabec, C. J. (2006). *Adv. Mater.*, *18*, 789.